The International Supercritical CO_2 Energy Technologies Symposium
March 2 - 5, 2026, Pittsburgh, PA
Poster #024

Design and Evaluation of a sCO_2 Pin-Fin Cold Plate for Motor Cooling

Ethan Neuwirth-Guerra[1], Alexander S. Rattner[1], Kathryn L. Kirsch[2], Malcolm Macdonald[2], Brian M. Fronk[1]

The Pennsylvania State University
Department of Mechanical Engineering
University Park, PA 16802

RTX Technology Research Center
411 Silver Lane
East Hartford, CT 06118

ABSTRACT

Supercritical carbon dioxide (sCO_2) power cycles can simultaneously generate power at high temperature and pressure while providing effective cooling for electronic components on the low-pressure (near-critical) side. Near the critical point, sCO_2 has high volumetric heat capacity and other favorable thermophysical and transport properties, making it an attractive working fluid for compact, high-performance heat exchangers. This study presents the design, optimization, and evaluation of an additively manufactured multichannel pin-fin cold plate tailored for cooling of a motor with near-critical sCO_2. The design was developed through parametric thermal and hydraulic simulations using experimentally informed sCO_2 pin-fin correlations to address design challenges including flow maldistribution, thermal non-uniformity, and structural integrity under the required pressure for operation. The cold plate was then fabricated out of AlSi10Mg using laser powder bed fusion. Following hydraulic proof testing, the cold plate was evaluated over a range of near-critical operating conditions varying mass and heat flux in a dedicated sCO_2 flow facility. The thermal performance of the cold plate was then compared to existing correlations for pin arrays and supercritical fluids. Results highlight mechanisms and trends not captured by current models, driven by steep property gradients and complex flow interactions. The final design balances thermal performance, manufacturability, and temperature uniformity, offering insights for future near-critical sCO_2 thermal management.

INTRODUCTION

As demand for high-powered electronics and efficient energy systems grows, supercritical carbon dioxide (sCO_2) has emerged as a promising working fluid for Brayton power cycles [1] advanced thermal management [2], and waste heat recovery. Its high-volumetric capacity, favorable thermophysical properties near the critical point, and low environmental impact make it an attractive alternative to conventional single-phase and two-phase coolants. In the near-critical region sCO_2 exhibits steep, nonlinear variations in density, viscosity, specific heat, and other properties (Figure 1) that give rise to complex convective thermal transport that can either enhance or degrade heat transfer depending on operating conditions and geometry.

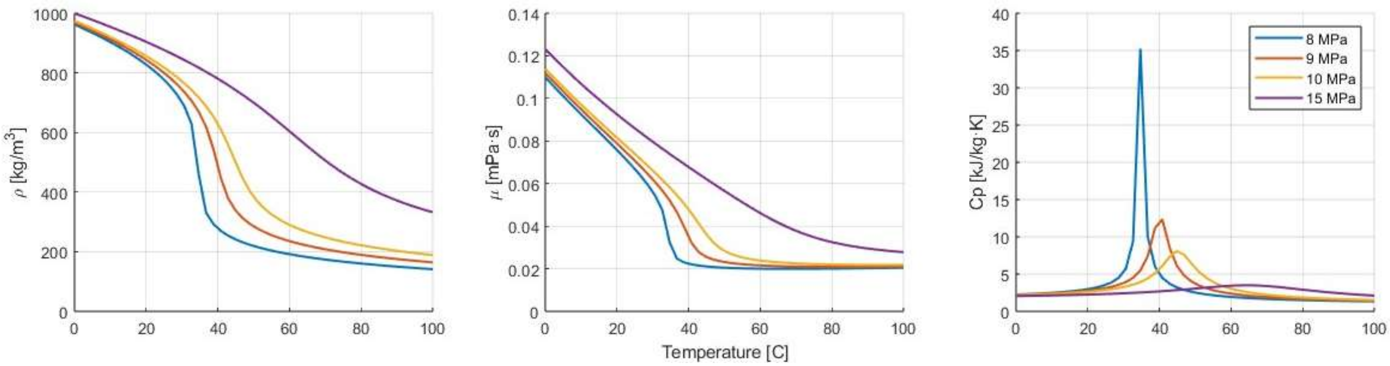

Figure 1: Thermophysical property variations for (a) density, (b) viscosity, and (c) specific heat of carbon dioxide near the critical point.

Prior studies on utilizing sCO_2 for thermal management have primarily focused on straight circular tubes or rectangular channels, advanced configurations, such as pin arrays and non-uniform channels, are gaining attention for their ability to disrupt boundary layers and promote mixing. These effects are particularly beneficial in the near-critical regime, where density-driven flow instabilities and enhanced thermal gradients can be amplified by geometric variation. This work introduces a single-pass multichannel cold plate designed and additively manufactured for power electronics cooling using near-critical sCO_2. The study combines parametric thermal modeling, structural optimization, and experimental validation to demonstrate uniform temperature distribution under for cooling of a simulated motor/generator using a supercritical coolant in a cylindrical cold plate.

METHODOLOGY AND MATERIALS

A parametrized thermal resistance network was used to design a cold plate consisting of alternating pin array channels and heat spreaders used for distributing heat flux. This model considered the key geometric features, including pin height, diameter, and pitches, channel and heat spreader width, wall thicknesses and number of parallel channels. A cross-section shown in Figure 2. Using the parametric model, feature dimensions were optimized to minimize weight while maintaining maximum surface temperatures within prescribed motor limits. The convective heat transfer coefficient of sCO_2 was estimated with a modified version of the Zukauskas et. al. [3] correlation for flow through a bank of tubes. A heat capacity normalizing factor following the approach of Jackson et al. [4] and Li et. al. [5] was added to account for property variation between the bulk and near-wall fluid temperatures, shown in Equations 1-6.

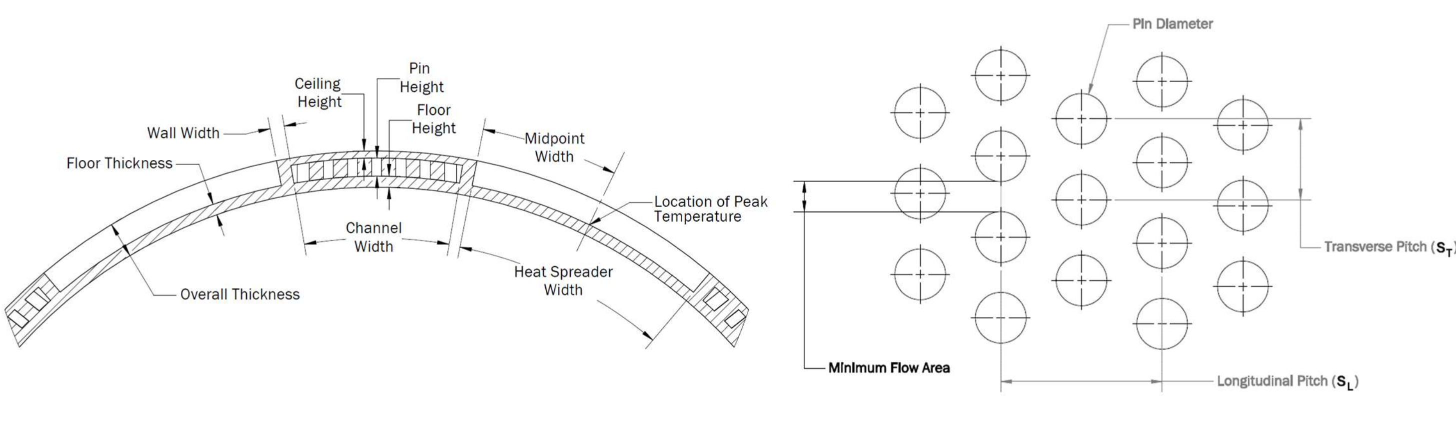

Figure 1: Cold plate geometric features used for optimization in parameterized model

$$\mathrm{Nu}_b = 0.35\left(\frac{\beta_t}{\beta_l}\right)^{0.2} Re_{A,min}{}^{0.6} Pr^{0.36}\left(\frac{Pr}{Pr_{wall}}\right)^{0.25}\left(\frac{\overline{C_p}}{C_{p,b}}\right)^{n} \quad (1)$$

$$\beta_L = \frac{S_L}{D_h},\ \beta_T = \frac{S_T}{D_h} \quad (2)$$

$$\overline{C_p} = \frac{i_w - i_b}{T_w - T_b} \quad (3)$$

$$n = 0.4\ ;\ \ T_b < T_w < T_{pc} \quad (4)$$

$$n = 0.4 + 0.2\left(\left(\frac{T_w}{T_{pc}}\right) - 1\right);\ \ T_b < T_{pc} < T_w \quad (5)$$

$$n = 0.4 + 0.2\left(\left(\frac{T_w}{T_{pc}}\right) - 1\right)\left(1 - 5\left(\left(\frac{T_w}{T_{pc}}\right) - 1\right)\right);\ \ T_{pc} < T_b < 1.2T_{pc} \quad (6)$$

With geometric features finalized, the design process advanced to iterative finite element analysis (FEA) coupled with fluid flow simulations to develop the header structures that serve as both flow distribution elements and load-bearing components. At an internal operating pressure of 7.8 MPa, the optimized header design provided uniform flow distribution, less than 2°C of wall temperature variation, and a structural factor of safety of 2.2.

Final modifications to the thermal, hydraulic, and mechanical design were implemented to ensure manufacturability via laser powder bed fusion. Fluid ports were intentionally oversized to allow post-machining and achieve the required surface finish for Swagelok compression fittings, enabling reliable integration with the test facility. To improve thermal contact with the heated motor simulator, an angled taper was incorporated on the cold plate's inner surface, matched by a corresponding taper on the heating element. Figure 3 illustrates the assembly steps following post-processing of the cold plate and integration of the heating component. The final design was fabricated using AlSi10Mg through laser powder bed fusion by an external vendor and assembled in the Penn State HEATER Lab.

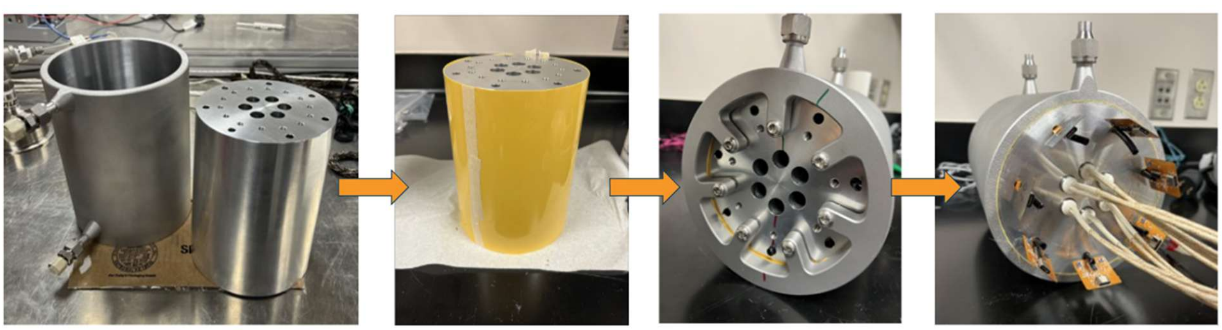

Figure 2: Assembly steps following post processing of the cold plate. A thermal gap pad material wrapped the heating element and secured into place using indexing features on the cold plate structure. The final image shows the installed heater cartridges (center) and profile temperature sensors (outer)

RESULTS AND DISCUSSION

After integration into the test facility, a series of experiments were conducted on the cold plate under varied operating conditions. Baseline cases with sCO_2 entering at gas-like and liquid-like temperatures and pressures were well predicted by the non-vortex shedding correlation by Rasouli et. al [6] with a mean average percent error (MAPE) of 22.2% for liquid-like and 27.9% for gas-like. Deviation was seen when the bulk temperature crossed the pseudo-critical temperature within the device. For these near-critical cases, inlet temperature was set at 99% of the pseudo-critical temperature in Kelvin at the corresponding pressure (T_{PC} = 306.7 K (33.5°C) and T_{IN} = 303.6 K (30.4°C)). Profile temperature sensors embedded in the heating element enabled calculation of the local heat transfer coefficient for each channel along the length of the test section.

Figure 4, shows calculated heat transfer coefficient versus length at heating powers ranging from 1600 W to 3000 W. Results indicate generally uniform heat transfer performance along the cold plate length, with minor variations attributed to flow imbalance, particularly in Channel 4, which is furthest from the inlet and outlet and exhibited the lowest heat transfer coefficient. Overall agreement to the modified Zukauskas et. al. correlation used for the design of the cold plate had a MAPE of 38.7%.

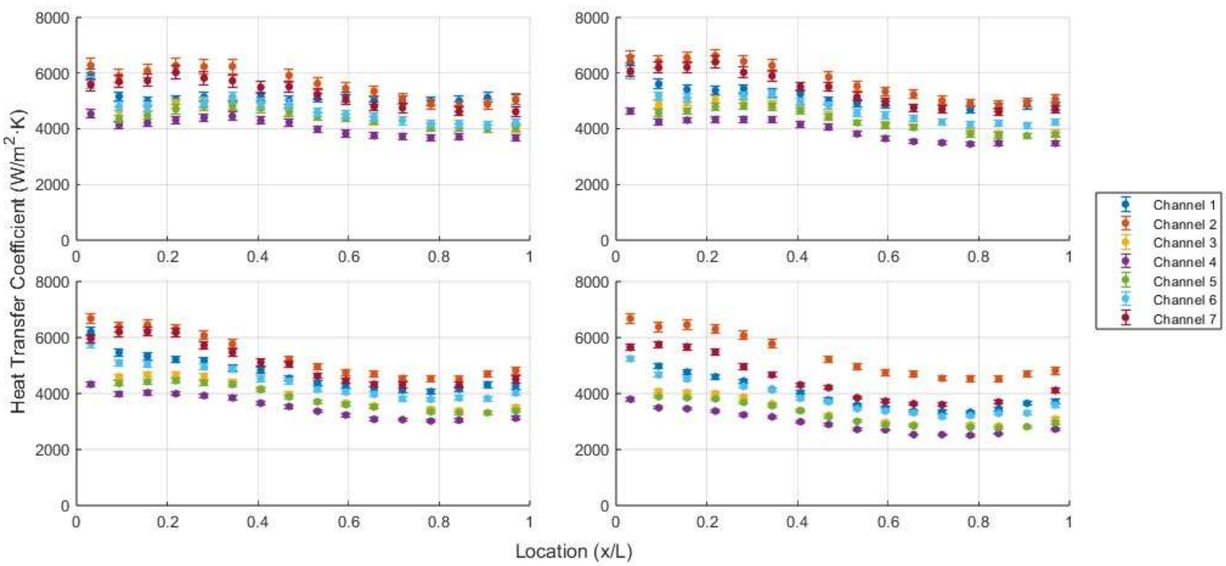

Figure 3: Local Heat Transfer Coefficients along the length of the cold plate for heat supplied of 1600W (Top-Left), 2000W (Top-Right), 2500W (Bottom-Left), and 3000W (Bottom-Right)

An additional analysis compared measured sCO_2 cooling performance to simulated cooling with water for similar operational conditions. Pumping power required for sCO_2 was selected as the baseline, and water performance was evaluated under the same pumping power and inlet temperature [2]. Figures 5 and 6 summarize these comparisons, using internal heating element temperature (i.e., maximum wall temperature) as the primary metric. Measured sCO_2 wall temperatures were plotted alongside predictions from a numerical thermal model developed for water.

Figure 5 shows that internal temperature rise along the cold plate is consistently greater for water than for sCO_2 across all near-critical cases. The difference is primarily due to the high specific heat capacity and near-isothermal behavior of sCO_2 in the near-critical region which limits the fluid temperature rise and promotes higher local heat transfer coefficients, minimizing wall temperature. The prevailing reason that explains this behavior is the near isothermal behavior near-critical sCO_2 experiences when crossing the pseudo-critical point. In contrast, water specific heat and local heat transfer coefficients are approximately constant, yielding a significant axial fluid temperature increase, reducing its heat transfer effectiveness.

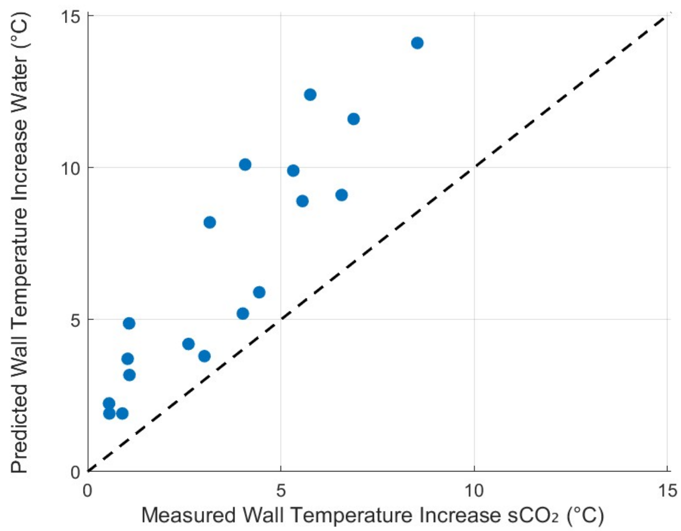

Figure 4: Internal Temperature Increase along length of channel. Comparison for sCO_2 and Water.

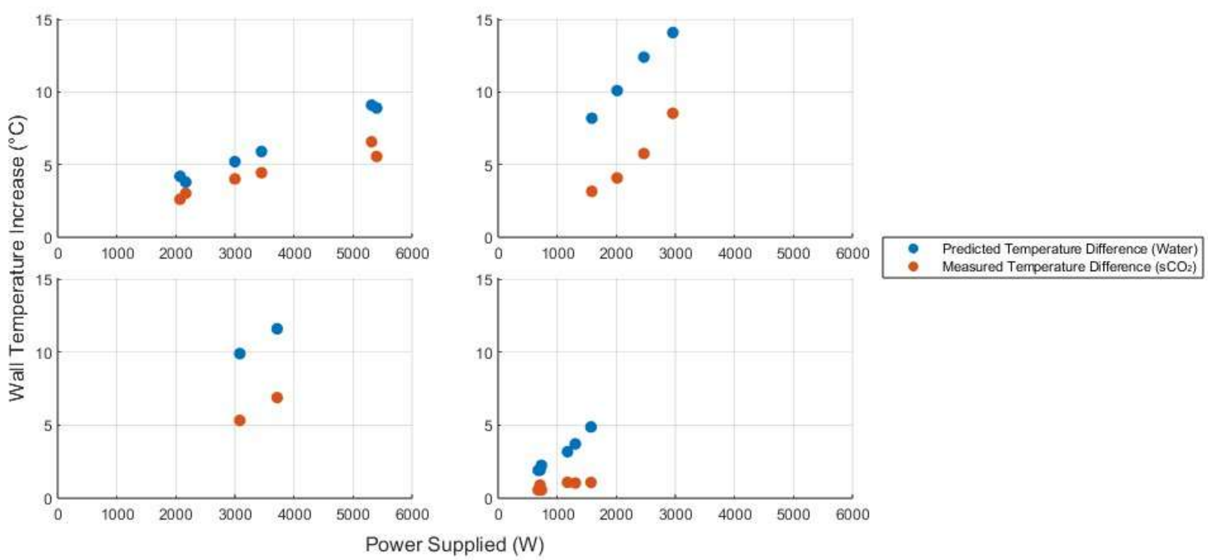

Figure 6: Internal Temperature Increase along length of channel separated by mass flow rate 300 kg/hr (top-left), 150 kg/hr (top-right), 100 kg/hr (bottom-left) and two-phase 150 kg/hr (bottom-right). Comparison for sCO_2 and Water

CONCLUSION

A jacketed cold plate was designed using integrated thermal, fluid, and structural models, fabricated via additive manufacturing, and experimentally validated under near-critical sCO_2 conditions. Testing demonstrated consistent local heat transfer performance along the channel length, mitigating localized thermal transport limitations while leveraging the near-isothermal behavior of sCO_2 compared to conventional single-phase coolants. These findings underscore the potential of near-critical sCO_2 for advanced electronics cooling applications, offering improved thermal uniformity and efficiency under high heat flux conditions.

ACKNOWLEDGEMENTS

The information, data, or work presented herein was funded in part by the Advanced Research Projects Agency-Energy (ARPA-E), U.S. Department of Energy, under Award Number DE-AR0001342. The views and opinions of authors expressed herein do not necessarily state or reflect those of the United States Government or any agency thereof.

REFERENCES

[1] Iverson, B. D., Conboy, T. M., Pasch, J. J., and Kruizenga, A. M., 2013, "Supercritical CO2 Brayton Cycles for Solar-Thermal Energy," Applied Energy, 111, pp. 957–970. https://doi.org/10.1016/j.apenergy.2013.06.020.

[2] Fronk, B. M., and Rattner, A. S., 2016, "High-Flux Thermal Management With Supercritical Fluids," Journal of Heat Transfer, 138(124501). https://doi.org/10.1115/1.4034053.

[3] Žukauskas, A., 1972, "Heat Transfer from Tubes in Crossflow," Advances in Heat Transfer, J.P. Hartnett, and T.F. Irvine, eds., Elsevier, pp. 93–160. https://doi.org/10.1016/S0065-2717(08)70038-8.

[4] Jackson, J. D., 2002, Consideration of the Heat Transfer Properties of Supercritical Pressure Water in Connection with the Cooling of Advanced Nuclear Reactors, Atomic Energy Press, China.

[5] Li, H., Kruizenga, A., Anderson, M., Corradini, M., Luo, Y., Wang, H., and Li, H., 2011, "Development of a New Forced Convection Heat Transfer Correlation for CO2 in Both Heating and Cooling Modes at Supercritical Pressures," International Journal of Thermal Sciences, 50(12), pp. 2430–2442. https://doi.org/10.1016/j.ijthermalsci.2011.07.004.

[6] Rasouli, E., Naderi, C., and Narayanan, V., 2018, "Pitch and Aspect Ratio Effects on Single-Phase Heat Transfer through Microscale Pin Fin Heat Sinks," International Journal of Heat and Mass Transfer, 118, pp. 416–428. https://doi.org/10.1016/j.ijheatmasstransfer.2017.10.105.